ISSN:2790-1688 DOI: 10.56028/aetr.4.1.110.2023

Analysis of slope management in Shangping

Yi Cao[1], Huaihai Li[1], Zhongshuai Liu[1], Chunyu Long[*]

[1]China Merchants Chongqing Communications Technology Research & Designinstitute Co.,Ltd., Chongqing, China

*Corresponding author e-mail: zbx724@qq.com

Abstract. To ensure the stability of the slope in Shangping, 5 monitoring sections and 17 monitoring points were set up on site. The most dangerous sliding profile of the slope was determined through data analysis; the stability coefficient of the slope was 1.03 by numerical calculation, which did not meet the engineering requirements and indicated that the slope was in an unstable state; the slope reinforcement plan of "anti-slip pile + anchor + drainage cut-off" was formulated by combining the monitoring data and simulation results, and the stability coefficient of the slope after reinforcement was 1.28 by numerical calculation, which met the reinforcement requirements of the project and indicated that the reinforcement plan was feasible. The stability coefficient is 1.28, which is 24.3% higher than that before reinforcement, which meets the reinforcement requirements and indicates that the reinforcement plan is feasible.

Keywords: monitoring; stability; anti-slip piles; anchors; reinforcement.

1. Introduction

The topography and terrain in Sichuan and Chongqing areas are complex, and the problem of slope hazards is prominent, which has been as one of the important factors affecting the safety of infrastructure. For a long time, slope hazards have also been a hot issue in the field of geotechnical engineering, and experts and scholars at home and abroad have carried out many researches. Zhao Minghua et al [1] proposed a theoretical calculation method of safety coefficient for rocky slopes and verified the reasonableness of the mechanical analysis model of rocky slopes and its analytical solution of safety coefficient with engineering examples; Yao Maohong et al [2] considered the model of rainfall infiltration of slopes under the action of saturated zone seepage and air pressure and derived the expression of its slope stability coefficient; Su Zhenning et al [3] proposed a three-dimensional slope stability analysis based on finite element elastic-plastic stress field and limit Xu Peng et al [4] used limit analysis to analyze the effects of load, interlayer shape and interlayer strength on slope stability; Zhang Kai et al [5] proposed a slope stability prediction model based on LightGBM algorithm and evaluated the generalization performance of the model; Li Yang et al [6] studied the force and deformation of double-row anti-slip piles under various forms of pile placement based on model tests and theoretical analysis. Deng Shirong et al [7] proposed a widened anti-slip pile structure at the top of the embedded section and derived the formulae for calculating the internal force, displacement and ground reaction force; Chen Jianfeng et al [8] combined particle image velocimetry to reveal the mechanism of the influence of anchorage length on the sliding surface and anti-slip capacity of homogeneous slopes; Sun et al [9] proposed a new pile spacing calculation considering end-bearing soil arch and friction soil arch and established a pile spacing control method. method and established the pile spacing control equation; Huang et al [10] discussed the differences between the calculation results of free pile bottom, articulated pile bottom and fixed pile bottom, and proposed the risk of wrong bracket selection; Lu et al [11] analyzed the effects of anchors with different burial depths, anti-slip piles with different depths, and different anti-slip pile reinforcement locations on slope reinforcement.

As a common form of reinforcement for slopes, antiskid piles and anchors play an important role in preventing slope collapse and protecting infrastructure safety. In this paper, the stability state of the slope before reinforcement is analyzed, and the slope reinforcement scheme is formulated with the analysis results. The research results have important guidance and reference for similar projects.

ISSN:2790-1688 DOI: 10.56028/aetr.4.1.110.2023

2. Project Overview

The slope is located in Shangping Village, Shashi Town, Yunyang County, Chongqing, and is a tectonic denudation of low mountain landforms, micro-geomorphology for the slope, the terrain is high in the north and low in the south, the plane form is generally slightly "semi-elliptical"; the longitudinal length is about 84 m, the horizontal width is about 101 m, the thickness of the deformation body is 3 to 18 m, the average thickness is about 11 m, the area is about 0.76×104 m2, the volume is about 8.36×104 m3, the height of the shear outlet at the front edge is 693 m, the height of the back edge is 747 m, the relative height difference is about 54 m, and the deformation direction is 213°. The survey area has a subtropical monsoon climate with an average annual rainfall of 1,145.1 mm; surface water flow in the area belongs to the Yangtze River system, mainly recharged by atmospheric rainfall and subject to seasonal influence; groundwater type is mainly loose soil type pore diving and bedrock fracture water; the front edge of the landslide area is bounded by the lower slope of the construction right-of-way, the rear edge by the tension cracks around the house, the west side by the surface ditch, and the east side by the sliding under the frustration The area is bounded by the surface ditch on the west side and the sliding deflection on the east side. The overall appearance of the deformation is shown in Figure 1.

Figure 1. Full view of the deformed body.

3. Slope stability analysis

3.1 Monitoring Analysis

On August 23, 2022, multiple cracks appeared at the back edge of the slope at 28 m, with the maximum crack width reaching 40 cm and height difference of 67 cm; on August 25, the site investigation found that the cracks showed a continuous development trend and gradually penetrated, multiple longitudinal cracks were newly found on the slope surface of the tertiary slope, and transverse cracks appeared on the platform. In order to ensure the stability state of the project, a total of 5 monitoring sections and 17 monitoring points were arranged on the slope since August 24, 2022, as shown in Figure 2.

ISSN:2790-1688 DOI: 10.56028/aetr.4.1.110.2023

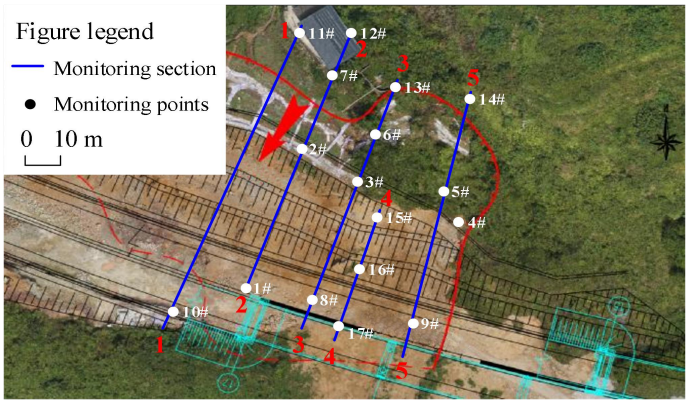

Figure 2. Monitoring layout.

The typical monitoring points in the upper, middle and lower parts of the slope are selected for analysis, and it is found that the slope displacement changes show a trend of increasing first, then stabilizing and then increasing again, and the specific data changes are shown in Figure 3.

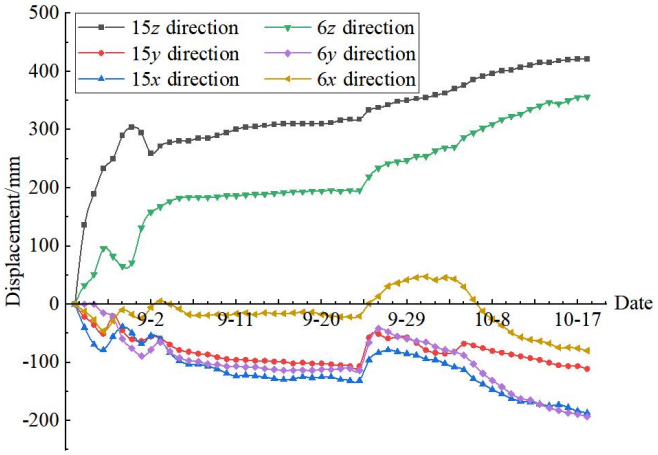

（a）6# and 15#

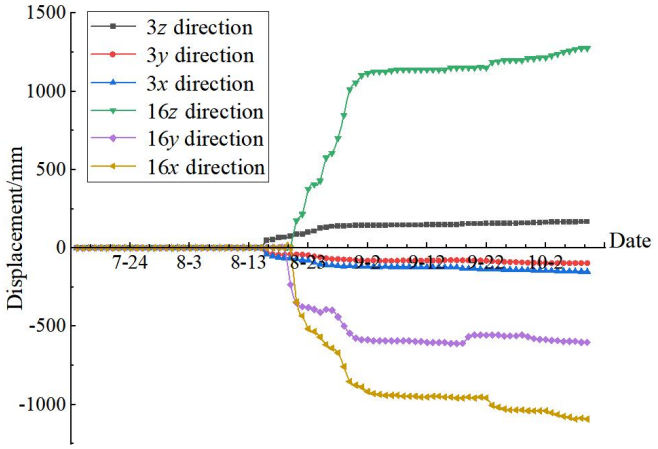

（b）3# and 16#

ISSN:2790-1688 DOI: 10.56028/aetr.4.1.110.2023

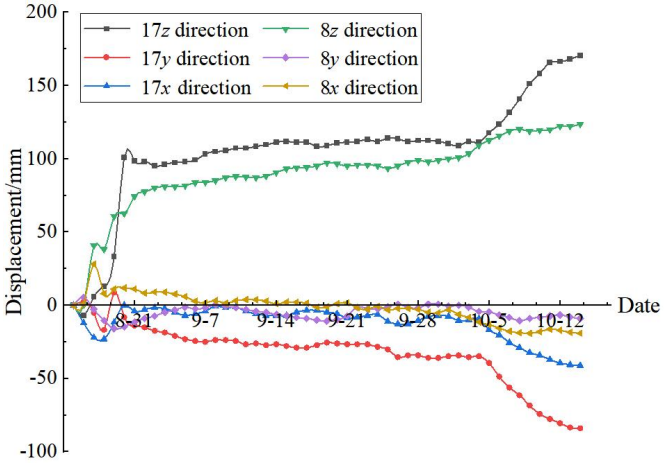

（c）8# and 17#

Figure 3. Changes in data at monitoring points.

It can be seen from Figure 3: 15# monitoring points in the upper part of the 4-4 section, 16# monitoring points in the middle and 17# monitoring points in the lower part have the largest displacement deformation in three directions, and the displacement deformation in the z-direction is positive and the displacement deformation in the y-direction is negative, indicating that the slope has the tendency to slide downward, and the displacement deformation in the x-direction is negative, indicating that the landslide has the tendency to misalign and squeeze in the direction of the 3-3 section. Therefore, the topography of the slope is considered. Therefore, considering the topography and geomorphology of the slope and combining with the results of data changes of monitoring points, section 4-4 is determined as the most dangerous profile of landslide.

3.2 Stability analysis

3.2.1 Parameter determination and model construction.

The analysis of the most dangerous profile of the landslide was carried out, and the geological structure of section 4-4 was obtained from the site survey as shown in Figure 4.

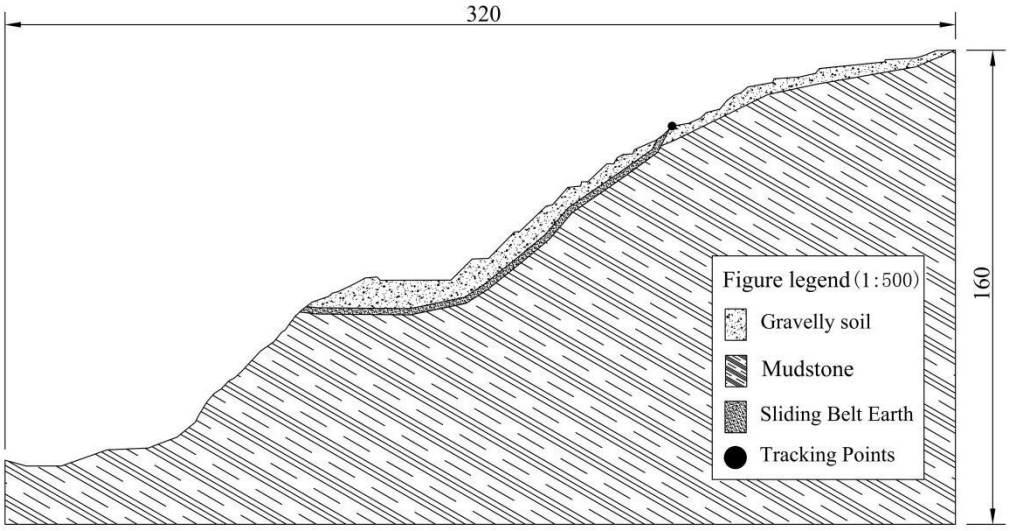

Figure 4. 4-4 Cross-sectional geological structure((unit: m).

The physical and mechanical parameters of the geotechnical body in section 4-4 measured by indoor and outdoor tests are shown in Table 1.

Table 1. Physical and mechanical parameters.

ISSN:2790-1688 DOI: 10.56028/aetr.4.1.110.2023

Category	Severe /(kN.m-3)	Cohesion /kPa	Friction angle/(°)	Modulus of elasticity/MPa	Poisson's ratio
Gravelly soil	18.5	14.7	11.14	16	0.17
Mudstone	25.3	230	35	250	0.37
Sliding Belt Earth	21.2	11.09	10.02	15	0.3

A finite element analysis model is established for section 4-4, as shown in Figure 5, and the model adopts the elasto-plastic principal structure model and Moore-Coulomb yield criterion. The boundary conditions of the model are: horizontal displacement constraints are imposed on the left and right boundaries, horizontal and vertical displacement constraints are imposed on the bottom surface, and the rest are free boundaries. CPE4 unit type is used for all the geotechnical bodies of the side slopes.

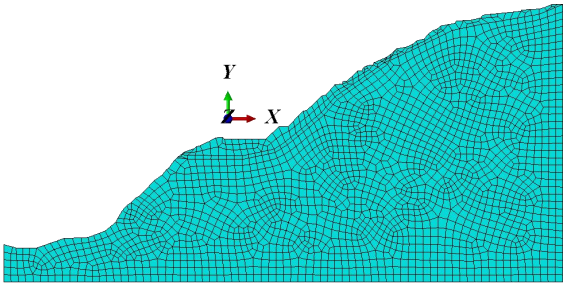

Figure 5. Finite element model.

3.2.1 Stability evaluation.

The average stress cloud of the slope is shown in Fig. 6 and the displacement cloud is shown in Fig. 7 from the numerical analysis.

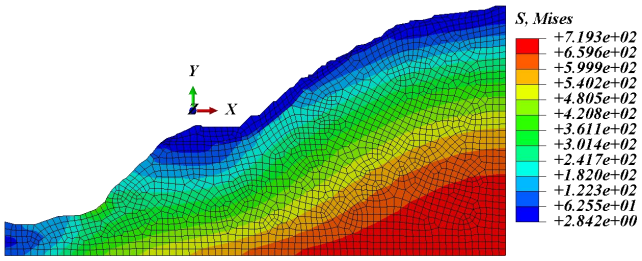

Figure 6. Average stress cloud diagram.

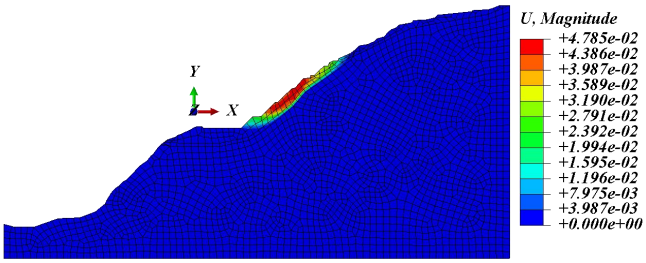

Figure 7. Displacement cloud map.

From Figs. 6~7, it can be seen that: the average stress of the slope is mainly concentrated in the mudstone region of the lower soil layer, and the average stress in the upper gravelly soil region is smaller; the displacement deformation of the slope is mainly concentrated in the gravelly soil region of the upper soil layer in the middle of the slope, while the displacement deformation in other regions is smaller.

ISSN:2790-1688 DOI: 10.56028/aetr.4.1.110.2023

In order to determine the stability state of the slope, the tracking point in Figure 1 is used as the study point, and the inflection point where the displacement of the characteristic point appears is used as the slope stability evaluation standard [12, 13], and the calculated slope stability coefficient change curve is shown in Figure 8.

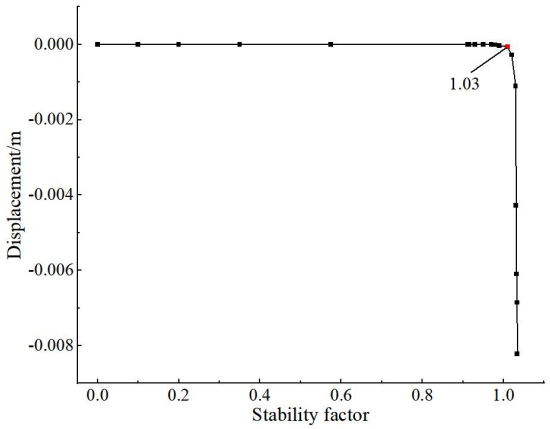

Figure 8. Stability coefficient change curve before reinforcement.

It can be seen from Figure 8: the stability coefficient of the slope before treatment is 1.03, while the code requires the stability coefficient of the slope to be 1.2~1.3 under normal working conditions, which does not meet the code requirements, indicating that the slope is in an unstable state and needs to be reinforced for treatment.

4. Governance Analysis

4.1 Governance program

After discussion at the technical proposal review meeting, combined with monitoring data and slope stability calculation results, it was decided to adopt the reinforcement plan of "anti-slip pile support + anchor rod + drainage interception", with anti-slip pile support on the first level platform, pile spacing 4 m, pile section 1.5×2 m, using C30 cast-in-place concrete anti-slip pile; the first to fourth level slopes are protected with anchor rod. Protection, 12 m long anchors are used for the first and fourth grade slopes, 20 m long anchors are used for the second and third grade slopes, and the angle with the horizontal plane is 20°; the slope body is equipped with elevated slope drainage holes, and the slope platform is equipped with intercepting ditch and additional intercepting ditch to drain the surface water of the slope body to the outside of the slope area. The specific scheme is shown in Figure 9.

The physical and mechanical parameters of the reinforcement materials in the reinforcement scheme are shown in Table 2.

Table 2. Physical and mechanical parameters of reinforced materials.

Category	Severe /(kN.m-3)	Cohesion /kPa	Friction angle/(°)	Modulus of elasticity/MPa	Poisson's ratio
Poisson's ratio	24	—	—	30 000	0.2
Anchor rods	—	—	—	200 000	0.25

ISSN:2790-1688 DOI: 10.56028/aetr.4.1.110.2023

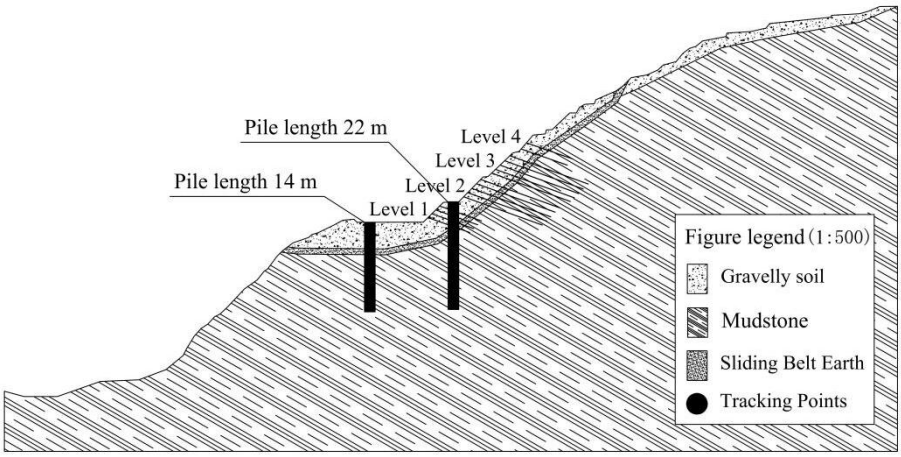

Figure 9. Schematic diagram of the reinforcement scheme.

4.2 Evaluation of results

The average stress cloud of the reinforced slope after numerical analysis is shown in Fig. 10, and the displacement cloud is shown in Fig. 11. Taking the tracking point in Fig. 1 as the study point, the simulation obtained the change curve of slope stability coefficient after reinforcement as shown in Fig. 12.

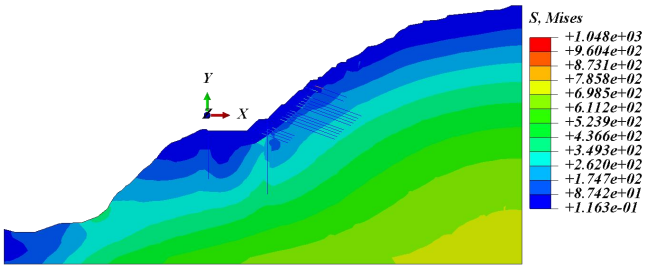

Figure 10. Average stress cloud diagram.

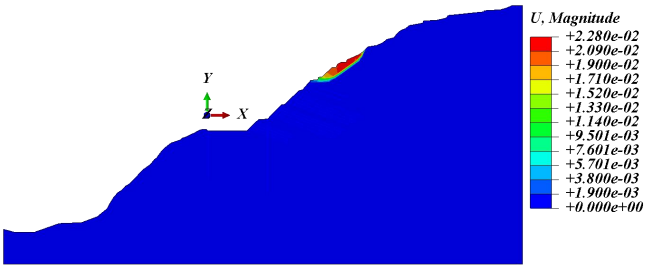

Figure 11. Displacement cloud map.

From Fig. 10, it can be seen that: the overall average stress of the slope is significantly reduced relative to that before reinforcement, and the anchors inserted into the upper part of the slope body are obviously stressed; from Fig. 11, it can be seen that: the displacement-deformation area of the slope has changed significantly, and the displacement range and size are significantly reduced relative to that before reinforcement, which indicates that the support structure has played an effective reinforcement role and blocked the sliding deformation of the upper soil layer of the slope; from Fig. 12, it can be seen that. The stability coefficient of the slope after reinforcement is 1.28, which is improved by 24.3% relative to that before reinforcement, meeting the reinforcement requirements in the specification, indicating that the reinforcement scheme is feasible.

ISSN:2790-1688 DOI: 10.56028/aetr.4.1.110.2023

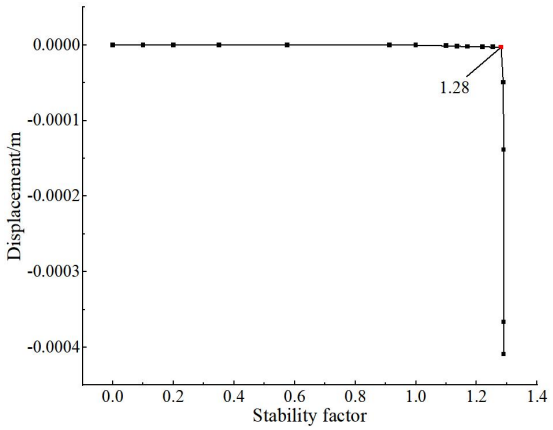

Figure 12. Change curve of slope stability coefficient after reinforcement.

5. Conclusion

(1) The monitoring data shows that section 4-4 is the most dangerous profile of the slope; the stability coefficient of the slope before reinforcement is 1.03, which does not meet the requirements of engineering specifications and indicates that the slope is in an unstable state.

(2) The stability coefficient of the reinforced slope is 1.28, which is 24.3% higher than that before reinforcement and meets the requirements of engineering specifications.

(3) The stability coefficient of the slope after reinforcement by "anti-slip pile support + anchor + drainage cut-off" meets the requirements of the project, which indicates that the reinforcement plan is feasible.

Acknowledgments

This work was financially supported by Chongqing Science and Technology Bureau Project （cstc2022ycjh-bgzxm0258） fund.

References

[1] M. H. Zhao, J. Y. Liu, H. Zhao, et al. Stability analysis of rocky slopes based on MSDP criterion, Journal of Rock Mechanics and Engineering. 2022, 41 (1) 10-18.

[2] M. H. Yao, Ti. L. Chen, R. Fan, et al. Slope stability under heavy rainfall conditions considering air pressure and seepage, Journal of Shanghai Jiaotong University. 2022, 56 (6) 739-745.

[3] Z. N. Su, L. T. Shao. Three-dimensional slope stability based on finite element limit equilibrium method, Journal of Engineering Science. 2022, 44 (12) 2048-2056.

[4] P. Xu, N. L. Shang, J. J. Bao, et al. Stability of slopes with weak inclusions by limit analysis, Journal of Southwest Jiaotong University. 2022, 57 (4) 919-925.

[5] K. Zhang, K. Zhang. Research on slope stability prediction based on LightGBM algorithm, Chinese Journal of Safety Science. 2022, 32 (7) 113-120.

[6] Y. Li, Y. L. Nan, H. C. He, et al. Model test of double-row anti-slip piles in loess soil, Journal of Safety and Environment. 2022, 22 (3) 1315-1322.

[7] S. Y. Deng, S. G. Xiao. Calculation method of widening type anti-slip pile at the top of embedded section, Chinese Journal of Geological Hazards and Prevention. 2022, 33 (4) 84-91.

[8] J. F. Chen, X. P. Guo, D. Tian,et al. Study on the effect of anchorage length of anti-slip pile on sliding surface and anti-slip capacity of homogeneous slope, Journal of Tongji University (Natural Science Edition). 2022, 50 (1) 42-49.

[9] C. J. Sun, J. Q. Yu, M. M. Liu, et al.Analysis of pile space of anti-slide piles, Hans Journal of Civil Engineering. 2021, 10 (1) 1-11.

ISSN:2790-1688 DOI: 10.56028/aetr.4.1.110.2023
[10] C. X. Huang, Y. Y. Zhao, J. Wu, et al.Design risk of incorrect selection of bottom support of anti-slide pile or pile wall, Hans Journal of Civil Engineering. 2021, 10 (4) 368-373.

[11] B. S. Lu, F. SONG, Y. T. Jin, et al.Stability analysis and reinforcement technology study of a highway slope in Cambodia, Hans Journal of Civil Engineering. 2021, 10 (5) 419-427.

[12] W. J. Sun, G. X. Wang, L. L. Zhang. Slope stability analysis by strength reduction method based on average residual displacement increment criterion, Bulletin of Engineering Geology and the Environment. 2021, 80 (6) 4367-4378.

[13] S. Y. Zhao, Y. R. Zheng, Y. F. Zhang. Exploration of the criterion of slope instability in the finite element strength reduction method, Geotechnics. 2005, 26 (2) 332-336.